

Gain equation for a free-electron laser with a helical wiggler and ion-channel guiding

Mahdi Esmailzadeh

Department of Physics, Iran University of Science and Technology, Tehran, Iran

Hassan Mehdian

Department of Physics, Teacher Training University, and Tarbiat Modaress, Tehran, Iran

Joseph E. Willett

Department of Physics and Astronomy, University of Missouri–Columbia, Columbia, Missouri 65211
(Received 30 January 2001; revised manuscript received 16 August 2001; published 7 December 2001)

The theory of ion-channel guiding in a helical wiggler is presented. Electron motion in the combined ion electrostatic and wiggler magnetostatic fields is analyzed in the absence of the radiation field. The Φ function that determines the rate of change of axial velocity with energy is derived and studied numerically. A detailed analysis of the pendulum equation and the gain equation in the low-gain-per-pass limit are presented. It is shown that the gain for stable group I orbits is positive, while for group II orbits the gain is negative in the negative mass regime and positive in the positive mass regime.

DOI: 10.1103/PhysRevE.65.016501

PACS number(s): 41.60.Cr, 52.59.Px

I. INTRODUCTION

A relativistic electron beam can be effectively confined in the transverse direction by use of an ion channel. First a plasma channel must be created, e.g., by the passage of a uv-laser beam through a gas. The electron beam may then be injected into the plasma channel to remove the plasma electrons by electrostatic repulsion. With an ion channel thereby formed, the beam electrons are electrostatically attracted to and confined transversely by the positive ions. The ion-channel radius should be of the order of the electron-beam radius and the ion density should be less than the electron density.

The use of ion-channel guiding in a free-electron laser (FEL) offers a number of advantages. It is a less expensive alternative to quadrupole or solenoidal magnetic guiding because of lower capital and operating costs [1]. Also, it permits beam currents higher than the vacuum limit [2]. A serious obstacle to intense electron beam transport with magnetic guiding is the transverse beam breakup instability. This instability may be effectively suppressed by ion-channel guiding [3]. Emittance growth due to scattering may also be suppressed [4]. Substantial gain enhancement may be obtained by operating with the ion-channel frequency near the wiggler frequency [5]. In a recent paper, Jha, Kumar, and Pande [6] have proposed that an FEL be operated at the ion-channel betatron frequency. This would offer the advantage of continuous tuning by varying the ion-channel density.

The purpose of the present paper is to extend the analysis of electron motion in a helical wiggler with ion-channel guiding and to derive the gain formula in the low-gain-per-pass limit. A modification of the method of Jha and Kumar [5] is employed. In Sec. II the Φ function that determines the rate of change of axial velocity with energy is investigated. Positive- and negative-mass regimes are identified and illustrated. In Sec. III the interaction of an electron with the radiation field is studied and a gain formula and pendulum equation are derived. In Sec. IV the results of a numerical

study of the gain are presented. It is shown that the gain in the negative-mass regime is negative according to the sign of Φ . In Sec. V a discussion and conclusions are presented.

II. Φ FUNCTION AND MASS REGIMES

In the idealized one-dimensional approximation, a helical wiggler magnetic field may be described by

$$\mathbf{B}_w = B_w(\hat{\mathbf{e}}_x \cos k_w z + \hat{\mathbf{e}}_y \sin k_w z), \quad (1)$$

where $k_w \equiv 2\pi/\lambda_w$ is the wiggler wave number. The electrostatic field generated by an ion channel, with its axis coincident with the wiggler (z) axis, may be written as

$$\mathbf{E}_i = 2\pi e n_i(\hat{\mathbf{e}}_x x + \hat{\mathbf{e}}_y y), \quad (2)$$

where n_i is the density of positive ions with charge e . The relativistic equation of motion for an electron with (rest) mass m and charge $-e$ moving with velocity \mathbf{v} in these combined fields is

$$\frac{d(\gamma m \mathbf{v})}{dt} = -e \left(\mathbf{E}_i + \frac{1}{c} \mathbf{v} \times \mathbf{B}_w \right). \quad (3)$$

Substituting Eqs. (1) and (2) into Eq. (3) leads to

$$\frac{d(\gamma m v_x)}{dt} = -2\pi e^2 n_i x + \frac{e v_z B_w}{c} \sin k_w z, \quad (4)$$

$$\frac{d(\gamma m v_y)}{dt} = -2\pi e^2 n_i y - \frac{e v_z B_w}{c} \cos k_w z, \quad (5)$$

$$\frac{d(\gamma m v_z)}{dt} = -\frac{e B_w}{c} (v_z \sin k_w z - v_y \cos k_w z). \quad (6)$$

Steady-state solutions of Eqs. (4)–(6) with constant axial velocity $v_z = v_{\parallel}$ (to first order in the wiggler amplitude) have been found to be [5]

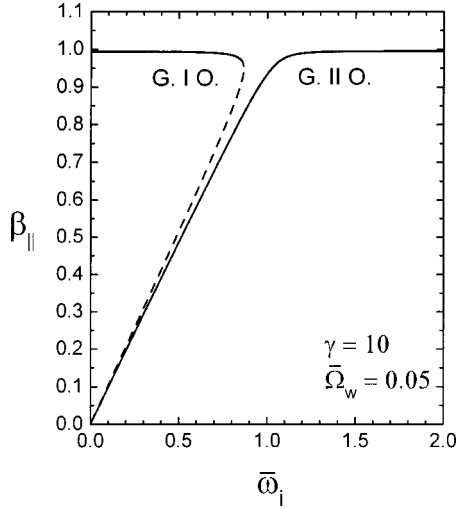


FIG. 1. Graph of the normalized axial velocity as a function of the normalized ion-channel frequency. The dashed line indicates the unstable group I orbits.

$$\beta_x = \frac{\bar{\Omega}_w \beta_{\parallel}^2}{\bar{\omega}_i^2 - \beta_{\parallel}^2} \cos k_w z, \quad (7)$$

$$\beta_y = \frac{\bar{\Omega}_w \beta_{\parallel}^2}{\bar{\omega}_i^2 - \beta_{\parallel}^2} \sin k_w z, \quad (8)$$

where $\bar{\Omega}_w \equiv eB_w / \gamma m c^2 k_w$, $\bar{\omega}_i^2 \equiv 2\pi e^2 n_i / \gamma m k_w^2 c^2$, $\beta_x \equiv v_x / c$, $\beta_y \equiv v_y / c$, and $\beta_{\parallel} \equiv v_{\parallel} / c$.

The Φ function that determines the rate of change of axial velocity with energy may be obtained as follows. Substituting Eqs. (7) and (8) into $\gamma^{-2} = 1 - \beta_x^2 - \beta_y^2 - \beta_z^2$ ($\beta_z = \beta_{\parallel}$) yields

$$\beta_{\parallel}^2 \left[1 + \frac{\bar{\Omega}_w^2 \beta_{\parallel}^2}{(\bar{\omega}_i^2 - \beta_{\parallel}^2)^2} \right] = 1 - \gamma^{-2}. \quad (9)$$

Implicit differentiation of Eq. (9) then leads to

$$\frac{d\beta_{\parallel}}{d\gamma} = \frac{1}{\gamma \gamma^2 \beta_{\parallel}} \Phi, \quad (10)$$

where $\gamma_{\parallel} \equiv (1 - \beta_{\parallel}^2)^{-1/2}$ and

$$\Phi = 1 - \frac{(1 + \gamma_{\parallel}^2) \bar{\Omega}_w^2 \bar{\omega}_i^2 \beta_{\parallel}^2}{(\bar{\omega}_i^2 - \beta_{\parallel}^2)^3 + 2\bar{\Omega}_w^2 \bar{\omega}_i^2 \beta_{\parallel}^2}. \quad (11)$$

Numerical solutions of Eqs. (9) and (11) are illustrated in Figs. 1 and 2, respectively, for a beam of electrons with $\gamma = 10$ (energy of 3.382 MeV) and $\bar{\Omega}_w = 0.05$.

Figure 1 shows β_{\parallel} as a function of the normalized ion-channel frequency $\bar{\omega}_i$ for group I orbits and group II orbits. Group I corresponds to the condition $\bar{\omega}_i < \beta_{\parallel}$ and group II corresponds to the condition $\bar{\omega}_i > \beta_{\parallel}$. The dashed line indicates unstable group I trajectories. The transition to orbital instability occurs at

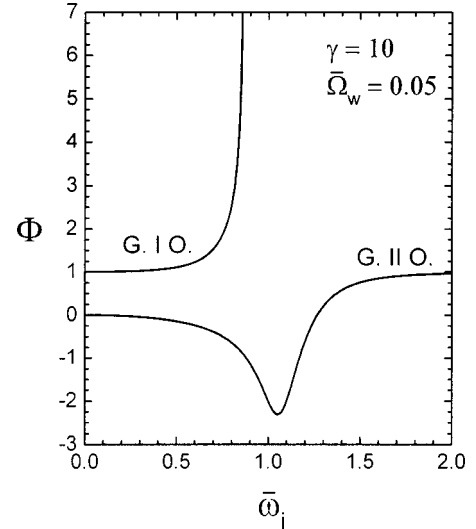


FIG. 2. Graph of Φ as a function of the normalized ion-channel frequency for the stable branch of group I orbits and group II orbits.

$$\bar{\omega}_i = (S_1 + T_1 + \beta_{\parallel}^2)^{1/2}, \quad (12)$$

where

$$S_1 = [\bar{\Omega}_w^2 \beta_{\parallel}^4 (\sqrt{8\bar{\Omega}_w^2 / 27 \beta_{\parallel}^2 + 1} - 1)]^{1/3}, \quad (13)$$

and

$$T_1 = -[\bar{\Omega}_w^2 \beta_{\parallel}^4 (\sqrt{8\bar{\Omega}_w^2 / 27 \beta_{\parallel}^2 + 1} + 1)]^{1/3}. \quad (14)$$

The numerical value of $\bar{\omega}_i$ at which transition to instability occurs is 0.8660 (for $\gamma = 10$ and $\bar{\Omega}_w = 0.05$).

Figure 2 shows Φ as a function of $\bar{\omega}_i$ for group I orbits (stable branch), and group II orbits. It is observed that for group I orbits Φ increases monotonically from unity at $\bar{\omega}_i = 0$, and exhibits a singularity at the transition to orbital instability [Eq. (12)]. The behavior of Φ for group II orbits is interesting because it is negative whenever

$$0 < \bar{\omega}_i < (S_2 + T_2 \beta_{\parallel}^2)^{1/2}, \quad (15)$$

where

$$S_2 = \left[\frac{\bar{\Omega}_w^2 \gamma_{\parallel}^2 \beta_{\parallel}^6}{2} (\sqrt{1 - 4\bar{\Omega}_w^2 \gamma_{\parallel}^2 / 27 + 1}) \right]^{1/3}, \quad (16)$$

and

$$T_2 = - \left[\frac{\bar{\Omega}_w^2 \gamma_{\parallel}^2 \beta_{\parallel}^6}{2} (\sqrt{1 - 4\bar{\Omega}_w^2 \gamma_{\parallel}^2 / 27 - 1}) \right]^{1/3}. \quad (17)$$

The negative Φ implies the existence of a negative-mass regime in which the axial velocity will increase with decreasing energy. The numerical value of $\bar{\omega}_i$ for group II orbits at which Φ goes to zero can be computed with the aid of Eqs. (9) and (15) and is found to be 1.2662 for parameters used in the figures. For $\bar{\omega}_i > 1.2662$, Φ is positive (positive-mass regime).

III. ELECTRON IN RADIATION FIELD

The electric and magnetic fields of the radiation in a wiggler may be represented by

$$\mathbf{E}_r = E_r(\hat{\mathbf{e}}_x \cos \xi - \hat{\mathbf{e}}_y \sin \xi), \quad (18)$$

$$\mathbf{B}_r = E_r(\hat{\mathbf{e}}_x \sin \xi + \hat{\mathbf{e}}_y \cos \xi), \quad (19)$$

where

$$\xi \equiv k_r z - \omega_r t + \phi; \quad (20)$$

k_r is the wave number, ω_r is the frequency, and ϕ is a phase constant. The equation of electron motion (3) in the presence of a radiation field can be written in the form

$$\begin{aligned} \frac{d(\gamma m v_x)}{dt} = & -2\pi n_i e^2 x + \frac{e v_z B_w}{c} \sin k_w z \\ & - e E_r (1 - \beta_z) \cos \xi, \end{aligned} \quad (21)$$

$$\frac{d(\gamma m v_y)}{dt} = -2\pi n_i e^2 y - \frac{e v_z B_w}{c} \cos k_w z + e E_r (1 - \beta_z) \sin \xi, \quad (22)$$

$$\begin{aligned} \frac{d(\gamma m v_z)}{dt} = & \frac{e B_w}{c} (v_y \cos k_w z - v_x \sin k_w z) \\ & + \frac{e E_r}{c} (v_y \sin \xi - v_x \cos \xi). \end{aligned} \quad (23)$$

For solution of these equations, we consider that for β_z close to 1 ($\gamma \gg 1$), the last terms in Eqs. (21) and (22) that are due to the electromagnetic radiation field can be neglected in comparison with others. Thus for β_z close to 1, the Eqs. (21) and (22) are the same as Eqs. (4) and (5), respectively. Therefore the transverse electron velocities in the presence of a radiation field are given by Eqs. (7) and (8) as well.

An expression for the axial velocity can be obtained as follows. Substituting Eqs. (7) and (8) into $\gamma^{-2} = 1 - \beta_x^2 - \beta_y^2 - \beta_z^2$ leads to

$$\beta_z = \left\{ 1 - \gamma^{-2} \left[1 + \frac{a_w^2 \beta_{\parallel}^4}{(\bar{\omega}_i^2 - \beta_{\parallel}^2)} \right] \right\}^{1/2}, \quad (24)$$

where

$$a_w \equiv \gamma \bar{\Omega}_w = e B_w / m c^2 k_w. \quad (25)$$

Expanding Eq. (24) for β_z close to 1 ($\gamma \gg 1$) yields

$$\beta_z \approx 1 - \frac{\gamma^{-2}}{2} \left[1 + \frac{a_w^2 \beta_{\parallel}^4}{(\bar{\omega}_i^2 - \beta_{\parallel}^2)^2} \right]. \quad (26)$$

This is the normalized axial velocity (v_z/c) in presence of the radiation field.

The energy exchange between an electron and the radiation field is given by

$$\dot{\gamma} = -(e/mc) \boldsymbol{\beta} \cdot \mathbf{E}_r. \quad (27)$$

Substituting Eqs. (7), (8), and (18) into Eq. (27) yields

$$\dot{\gamma} = - \frac{e E_r}{mc} \frac{\bar{\Omega}_w \beta_{\parallel}^2}{(\bar{\omega}_i^2 - \beta_{\parallel}^2)} \cos(k_w z + \xi). \quad (28)$$

Using a first-order approximation for z , $z = v_{\parallel} t = c \beta_{\parallel} t$, Eq. (28) may be written in the form

$$\dot{\gamma} = - \frac{e E_r}{mc} \frac{\bar{\Omega}_w \beta_{\parallel}^2}{(\bar{\omega}_i^2 - \beta_{\parallel}^2)} \cos(\Omega t + \xi), \quad (29)$$

where $\Omega \equiv (k_r + k_w) v_{\parallel} - \omega_r$.

The phase ϕ in Eq. (29) determines the initial position of the electron relative to the optical wave. Averaging this equation over all phases yields $\langle \dot{\gamma} \rangle_{\phi} = 0$; therefore, to first order there is no net transfer of energy between the electron beam and optical wave. The second-order correction will consist of accounting for the fact that as an individual electron (with phase ϕ) gains or loses energy, its position relative to unperturbed position ($z = v_{\parallel} t = c \beta_{\parallel} t$) is advanced or retarded. Therefore, the unperturbed position, $z = c \beta_{\parallel} t$, must be replaced by

$$z = c \beta_{\parallel} t + c \int_0^t \Delta \beta_z(t') dt', \quad (30)$$

where $\Delta \beta_z(t) = \int_0^t \dot{\beta}_z(t') dt'$ is the change of β_z relative to the unperturbed condition.

Differentiating Eq. (26) with respect to time and eliminating $\dot{\gamma}$ by use of Eq. (29) then yields

$$\dot{\beta}_z = - \frac{e E_r}{mc \gamma^4} \frac{a_w \beta_{\parallel}^2}{(\bar{\omega}_i^2 - \beta_{\parallel}^2)} \left[1 - \frac{a_w^2 \beta_{\parallel}^4}{(\bar{\omega}_i^2 - \beta_{\parallel}^2)^3} \right] \cos(\Omega t + \phi). \quad (31)$$

This equation may be substituted into Eq. (30) to obtain

$$z(t) = c \beta_{\parallel} t + \frac{c D}{\Omega} [\cos(\Omega t + \phi) - \cos \phi + \Omega t \sin \phi], \quad (32)$$

where

$$D = \frac{e E_r}{mc \gamma^3} \frac{\bar{\Omega}_w \beta_{\parallel}^2}{(\bar{\omega}_i^2 - \beta_{\parallel}^2) \Omega} \left[1 - \frac{a_w^2 \beta_{\parallel}^6}{(\bar{\omega}_i^2 - \beta_{\parallel}^2)^3} \right]. \quad (33)$$

The substitution of Eq. (32) into Eq. (28) yields

$$\begin{aligned} \dot{\gamma} = & - \frac{e E_r}{mc} \frac{\bar{\Omega}_w \beta_{\parallel}^2}{(\bar{\omega}_i^2 - \beta_{\parallel}^2)} \cos \left\{ (\Omega t + \phi) + \frac{(\omega_w + \omega_r) D}{\Omega} \right. \\ & \left. \times [\cos(\Omega t + \phi) - \cos \phi + \Omega t \sin \phi] \right\}, \end{aligned} \quad (34)$$

where $\omega_w \equiv c k_w$ and $\omega_r \equiv c k_r$. A comparison of Eq. (34) to Eq. (29) reveals that the perturbed condition consists of a phase slippage

$$\Delta\phi = \frac{(\omega_w + \omega_r)}{\Omega} [\cos(\Omega t + \phi) - \cos\phi + \Omega t \sin\phi]. \quad (35)$$

Since D is proportional to γ^{-3} and E_r , $\Delta\phi$ can be made arbitrarily small. Therefore, expanding the cosine term of Eq. (34) for $\Delta\phi \ll \pi$ leads to

$$\begin{aligned} \dot{\gamma} = & -\frac{eE_r}{mc} \frac{\bar{\Omega}_w \beta_{\parallel}^2}{(\bar{\omega}_i^2 - \beta_{\parallel}^2)} \left\{ \cos(\Omega t + \phi) - \sin(\Omega t + \phi) \right. \\ & \left. \times \frac{(\omega_w + \omega_r)D}{\Omega} [\cos(\Omega t + \phi) - \cos\phi + \Omega t \sin\phi] \right\}. \end{aligned} \quad (36)$$

Averaging over phase ϕ yields

$$\langle \dot{\gamma} \rangle_{\phi} = \frac{eE_r \bar{\Omega}_w \beta_{\parallel}^2 (\omega_w + \omega_r) D}{2mc (\bar{\omega}_i^2 - \beta_{\parallel}^2) \Omega} (\Omega t \cos \Omega t - \sin \Omega t). \quad (37)$$

Integrating the above equation over the electron transit time through the wiggler, the average change in γ per electron becomes

$$\begin{aligned} \langle \Delta\gamma \rangle_{\phi} = & \int_0^{T=L/v_{\parallel}} \langle \dot{\gamma} \rangle_{\phi} dt = \\ & -\frac{eE_r}{2mc} \frac{\bar{\Omega}_w \beta_{\parallel}^2 (\omega_w + \omega_r) D T^3 \Omega}{(\bar{\omega}_i^2 - \beta_{\parallel}^2)} g(\Omega T), \end{aligned} \quad (38)$$

where L is the FEL interaction length and

$$g(\Omega T) \equiv \frac{2 - 2 \cos \Omega T - \Omega T \sin \Omega T}{\Omega^3 T^3}. \quad (39)$$

The change of electromagnetic power in one transit is

$$\Delta P = -\frac{I}{e} mc^2 \langle \Delta\gamma \rangle_{\phi}, \quad (40)$$

where $I = en_b v_{\parallel}$ area is the average electron beam current and n_b is the density of the electron beam. Finally by using Eq. (38) under the assumption that the electrons are near resonance with the wave, [i.e., $\Omega = (k_r + k_w)c\beta_{\parallel} \rightarrow \omega_r \equiv 0$], the gain equation becomes

$$G = \frac{\Delta P}{P} = \frac{4\pi e^2 n_b L^3 \omega_w}{m(\gamma c \beta_{\parallel})^3} \frac{a_w^2 \beta_{\parallel}^4}{(\bar{\omega}_i^2 - \beta_{\parallel}^2)^2} F(\bar{\omega}_i) g(\Omega T), \quad (41)$$

where $P \equiv c(1/8\pi)(E_r^2 + B_r^2)$ area = $c(E_r^2/4\pi)$ area is the em power, and

$$F(\bar{\omega}_i) \equiv 1 - \frac{a_w^2 \bar{\omega}_i^2 \beta_{\parallel}^4}{(\bar{\omega}_i^2 - \beta_{\parallel}^2)^3 + a_w^2 \beta_{\parallel}^4 (\bar{\omega}_i^2 - \beta_{\parallel}^2)}. \quad (42)$$

Equation (41) is the gain equation for a free-electron laser with helical wiggler and ion-channel guiding in the low-

gain-per-pass limit. As it will be shown in Sec. IV, the existence of negative gain in the negative-mass regime is a new result that has not been previously reported for this type of free-electron laser.

The pondermotive phase or electron phase is defined as

$$\zeta \equiv (k_r + k_w)z - \omega_r t. \quad (43)$$

Differentiating Eq. (43) twice with respect to time, eliminating $\dot{\beta}_z$ by differentiating Eq. (26) with respect to time, and then using the exact form of $\dot{\gamma}$ [Eq. (28)] leads to

$$\ddot{\zeta} = -K^2 \cos(\zeta + \phi), \quad (44)$$

where

$$K^2 = (k_r + k_w) \frac{eE_r}{m\gamma^4} \frac{a_w \beta_{\parallel}^2}{(\bar{\omega}_i^2 - \beta_{\parallel}^2)} \left[1 - \frac{a_w^2 \beta_{\parallel}^6}{(\bar{\omega}_i^2 - \beta_{\parallel}^2)^3} \right]. \quad (45)$$

Equation (44) is the self-consistent pendulum equation that describes electron-photon interaction in a free-electron laser with helical wiggler and ion-channel guiding.

IV. NUMERICAL STUDY OF GAIN

If the normalized ion-channel frequency $\bar{\omega}_i$ is set equal to zero, Eq. (41) reduces to

$$G_0 = \frac{4\pi e^2 n_b L^3 \omega_w a_w^2}{m(\gamma c \beta_{\parallel})^3} g(\Omega T), \quad (46)$$

which is the gain equation for a helical wiggler FEL without an ion channel.

Figure 3 shows $\Delta \equiv G/G_0$, the ratio of gain with ion channel to gain without ion channel, as a function of $\bar{\omega}_i$ for $\beta_{\parallel} \equiv v_{\parallel}/c$ close to 1 ($\beta_{\parallel} > 0.95$). For group I orbits, the gain ratio Δ increases monotonically from unity at $\bar{\omega}_i = 0$ and becomes large (187) at the orbital instability, $\bar{\omega}_i = 0.866$. Therefore, gain enhancement is obtained relative to absence of the ion-channel guiding. For group II orbits if $\bar{\omega}_i < 1.027$, then $\beta_{\parallel} < 0.95$, and the condition of β_{\parallel} close to 1 (our condition or assumption for deviation of the gain equation) breaks down. The behavior of gain ratio Δ for this group is interesting because it is negative when $F(\bar{\omega}_i)$ is negative. The gain ratio Δ is equal to -182 at $\bar{\omega}_i = 1.027$, and goes to zero when $F(\bar{\omega}_i) = 0$ at $\bar{\omega}_i = 1.266$. For $\bar{\omega}_i > 1.266$ the gain ratio Δ becomes positive, goes to its maximum that is less than 1, and then starts decreasing to zero with increasing $\bar{\omega}_i$. As mentioned in Sec. II for group II orbits, the function Φ [Eq. (11)] is negative when $\bar{\omega}_i < 1.266$, and then becomes positive when $\bar{\omega}_i > 1.266$. Consequently the gain ratio Δ is negative when Φ is negative and is positive when Φ is positive.

Numerical consideration shows that if β_{\parallel} goes to 1, then $F(\bar{\omega}_i)$ [Eq. (39)] goes to Φ [Eq. (11)]. Therefore, with good approximation for β_{\parallel} close to 1, $F(\bar{\omega}_i)$ can be replaced by Φ in Eq. (41) to obtain

$$G = \frac{4\pi e^2 n_b L^3 \omega_w}{m(\gamma c \beta_{\parallel})^3} \frac{a_w^2 \beta_{\parallel}^4}{(\bar{\omega}_i^2 - \beta_{\parallel}^2)^2} \Phi g(\Omega T). \quad (47)$$

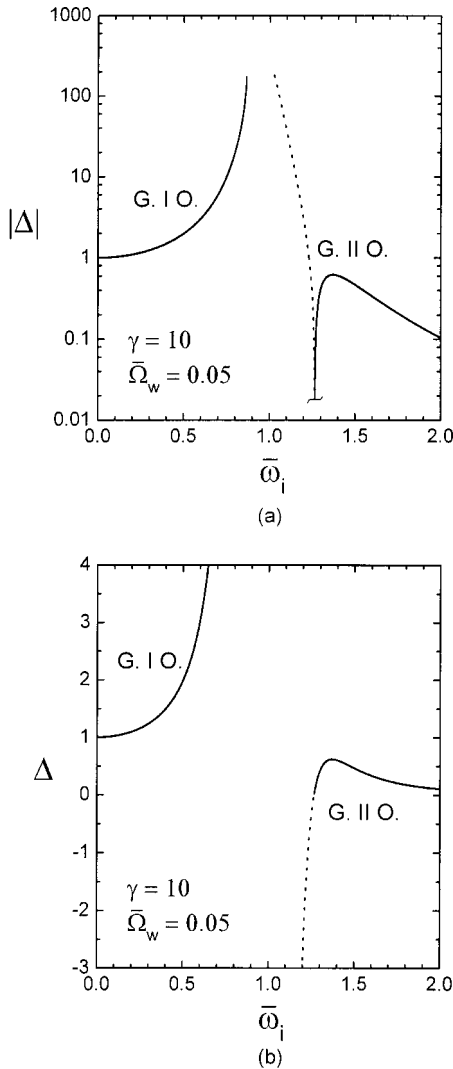


FIG. 3. (a) Graph of the absolute value of the gain ratio as a function of the normalized ion-channel frequency for $\beta_{||} > 0.95$. The dotted line indicates the negative part of the gain ratio for group II orbits. (b) Graph of a small region of the gain ratio in linear scale as a function of the normalized ion-channel frequency for $\beta_{||} > 0.95$. The dotted line indicates the negative part of the gain ratio for group II orbits.

Figure 4 shows the graphs of the absolute gain ratio, using Eqs. (41) and (47), for comparison. As this figure shows the graphs are the same as each other except near the peaks for which $\beta_{||} = 0.95$. This is expected because $\beta_{||} = 0.95$ is not very close to 1. The gain equation (47) is valid in the low-gain-per-pass limit with $\beta_{||}$ close to 1 ($\gamma \gg 1$), and is proportional to the Φ function in presence of an ion channel just as it is in the presence of an axial magnetic field [7]. Therefore, the gain is positive for positive-mass regime, ($\Phi > 0$), zero for zero-mass regime ($\Phi = 0$), and negative for negative-mass regime.

V. DISCUSSION AND CONCLUSIONS

The first successful test of ion-channel guiding was reported by Caporaso *et al.* in 1986 [8]. This technique was

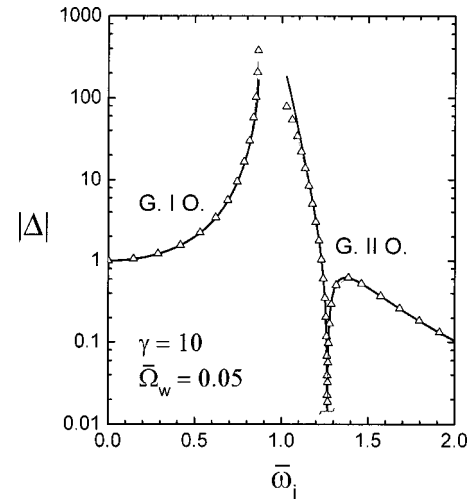


FIG. 4. Graphs of the absolute value of the gain ratio as a function of the normalized ion-channel frequency by using Eqs. (41) and (47) for $\beta_{||} > 0.95$. The solid lines indicate the absolute value of the gain ratio by using Eq. (41), and the symbol lines (triangles) indicate the absolute value of the gain ratio by using Eq. (47). As this figure shows, the two graphs are the same except at the peaks.

employed to transport a 10 kA electron beam through an advanced test accelerator. Preliminary free-electron laser experiments using an ion channel were carried out in 1989 by Ozaki *et al.* with only modest success. Their more recent experiment, carried out after extending the wiggler and reconfiguring the rf input, showed vast improvement in FEL performance [9].

Simulation studies of ion-channel guiding have provided an alternative to experimental testing. Ozaki *et al.* have developed a three-dimensional (3D) FEL simulation incorporating realistic beam transport effects. Yu, Sessler, and Whitlum [10] have reported that the use of ion-channel guiding together with beam conditioning greatly enhances FEL gain in the VUV and soft x-ray range. Their paper includes the results of 3D simulation for a 30-Å example that exhibits an order of magnitude increase in gain. Simulation studies by Jha and Wurtele [11] have also shown that significant gain enhancement can be obtained using ion-channel guiding. Their 3D simulation code includes space-charge effects that are important in low-energy electron beams.

Recently Chen, Liu, and Xie [12] have used particle modeling to study the setting up of an ion channel, its transient properties, and the factors affecting its performance. Their paper presents results of value for the development of an ion-channel FEL. If the beam electron density is smaller than the plasma density, there will be excess plasma electrons inside the channel that will cause the beam to be unstable. Their calculations show that oscillations of the ions and of the electron beam itself can exist. Under proper conditions, however, a pure ion channel with no oscillations can be established. It is very important to employ a high quality electron beam and to properly control the configuration of the ion channel.

On the basis of the experimental and simulation studies that have previously been carried out, we conclude that ion-

channel guiding is a viable alternative to the use of magnetic-field guiding in an FEL. It has a unique set of advantages as discussed in Sec. I. The spread in longitudinal velocity of the electron beam is detrimental to FEL performance. Also, limitations may be imposed by both electron-hose and ion-hose instabilities. Beam conditioning, although somewhat challenging, appears to be a method by which performance can be improved.

Jha and Kumar [5] have derived a simple analytical formula for the gain in a FEL with helical wiggler and ion-channel guiding. Their analysis predicts a substantial enhancement in the gain as the ion-channel frequency approaches the wiggler frequency. On the basis of our analysis, we conclude that a correction factor for their gain formula is required. It predicts, for example, that the gain can occur only in the positive-mass regime.

-
- [1] K. Takayama and S. Hiramatsu, *Phys. Rev. A* **37**, 173 (1988).
[2] Y. Seo, V. K. Tripathi, and C. S. Liu, *Phys. Fluids B* **1**, 221 (1989).
[3] P. Jha and P. Kumar, *Phys. Rev. E* **57**, 2256 (1998).
[4] T. P. Hughes and B. B. Godfrey, *Phys. Fluids* **27**, 1531 (1984).
[5] P. Jha and P. Kumar, *IEEE Trans. Plasma Sci.* **24**, 1359 (1996).
[6] P. Jha, P. Kumar, and K. Pande, *IEEE Trans. Plasma Sci.* **27**, 637 (1999).
[7] H. P. Freund, P. Sprangle, D. Dillenburg, E. H. da Jornada, B. Liberman, and R. S. Schneider, *Phys. Rev. A* **24**, 1965 (1981).
[8] G. J. Caporasa, F. Rainer, W. E. Martin, D. S. Prono, and A. G. Cole, *Phys. Rev. Lett.* **57**, 1591 (1986).
[9] T. Ozaki, K. Ebihara, S. Hiramatsu, Y. Kimura, J. Kishuro, T. Monaka, K. Takayama, and D. H. Whittum, *Nucl. Instrum. Methods Phys. Res. A* **318**, 101 (1992).
[10] L.-H. Yu, A. M. Sessler, and D. H. Whittum, *Nucl. Instrum. Methods Phys. Res. A* **318**, 721 (1992).
[11] P. Jha and J. S. Wurtele, *Nucl. Instrum. Methods Phys. Res. A* **331**, 447 (1993).
[12] X. Chen, S.-g. Liu, and W.-k. Xie, *Acta Electron. Sin.* **28**, 61 (2000).